INITIAL STAGES OF THE DEEP IMPACT COLLISION. P. H. Schultz, C. A. Eberhardy, and C. M. Ernst, Brown University, Department of Geological Sciences, 324 Brook Street, Providence, RI 02912-1846 (peter_schultz@brown.edu).

Introduction: The Deep Impact mission collided with Comet 9P/Tempel 1 on July 4, 2005. Observations from the flyby spacecraft, earth-based telescopes, and various probes provided complementary, although some times conflicting results. The goal here is to use laboratory-scale experiments to better understand the early-stage vapor/dust plume. Results have implications for understanding the early gas phases, chemical processing in the plume, energy partitioning (and balance) as well as the nature of the faint "first light" produced by the Deep Impact collision[1,2,3,4,5].

Experimental Design: The studies were performed at the NASA Ames Vertical Gun Range at NASA Ames Research Center. Projectiles 6.35mm in diameter (Pyrex, to ensure complete fragmentation) impacted with velocities ranging from 5 to 6km/s, all at an angle of 30° from the horizontal. A short-exposure (250ns) thermal imaging camera recorded the initial evolution of the vapor plume while high-speed spectrometers probed evolving conditions [see 6, 7]. This experimental design resembled observing conditions for the DI-IR spectrometer, which captured the initial plume as it passed a pixel exposed for 0.72s [1, 5]. The first experimental series addressed the evolution of the plume on and off the trajectory axis in order to understand contrasting processes within the vapor plume. The second series assessed the effect of porosity and layering in order to understand the provenance and evolution of different atomic and molecular emissions.

A range of surrogate targets were used: dolomite (solid and powdered); dolomite and sand mixtures; mixtures of dolomite and perlite; and layered targets with complex organic assemblages (e.g., sugar). Such surrogates allow tracking the relative proportion of atomic (e.g., Ca, Mg) and molecular species (CaO, MgO, CO_2, C_2). Emissions from these tracer components also can be used to examine the effects of porosity, mixtures, and surface layers on vapor conditions and evolution. All experiments were performed under a vacuum (0.5Torr) such that any atmospheric effects on the plume conditions are negligible.

Vapor Expansion: The vapor cloud travels downrange above the surface in an inertial frame that is decoupled from the rest of the impact. This momentum-driven component results from combination of two processes: downrange-directed shock heating and turbulent mixing with the jetting phase. The initial downrange speed of the vapor plume is not constant but rapidly decreases within 10 projectile diameters from the point of first contact (Fig. 1). The apparent deceleration results from non-isentropic expansion of the vapor at the earliest stages (as well as delayed emergence from the initial cavity). Shock rarefactions off the gas/vacuum interface appear slow the leading edge, similar to that observed for explosions in a vacuum [8]. This results in the redistribution of momentum and kinetic energy from the plume front back into the gas. Eventually adiabatic expansion controls expansion as the internal energy in the gas is converted to kinetic energy of expansion (along with lower densities and temperatures). The downrange horizontal component of velocity added to the radial gas expansion rate gives a net speed of 13.9 km/s, which is similar to the initial downrange plume speed of 12.7 km/s.

After about 100μs, lateral expansion rates asymptotically approach a constant value (u_{max} ~ 2.2 km/s) reflecting the complete conversion of the initial internal energy of the gas to kinetic energy of expansion in a vacuum (Fig. 1). The effect of the residual atmosphere in the chamber (~0.5 Torr) does not affect the plume until much later in time, after the gas has expanded to much greater dimensions [9].

While the position of emergence of the vapor plume from the target might be derived using the time since impact and speed extrapolated back to the target, this approach produces enigmatic results due to the initial high speed of the vapor. For example, if we had used just this late-stage speed of the plume front, the impact point would appear to be downrange from the actual impact. This insight has relevance to observations of the DI vapor plume.

Spectral Observations: Figure 2a provides a reference for the different fields of view. Because exposures lasted 50μs, each spectrum represents a time-integrated passage of the vapor plume passing through a 2.5cm field of view (FOV) at 8 km/s (Fig. 2a). Fibers coupled the telescopes to the spectrometers so that the spectra recorded data on common CCD's (2 on one, 3 on another). Four telescopes viewed each event from above through two 45° ports positioned uprange (but on each side of the trajectory axis ~45°) and looking downrange; a fifth telescope was positioned in the 45° port looking directly downrange (a viewing geometry similar to Deep Impact). Figure 2b shows the spectral evolution of the plume perpendicular to the trajectory and positioned ~ 10cm downrange (FOV's 6, 4, and 2) for an impact into a solid block of dolomite. Atomic lines become weaker relative to the molecular lines when viewed slightly off axis (FOV 4), but a weak Mg emission line at 418nm is observed. Far from the trajectory (FOV 2), molecular emission lines (CO, C_2) dominate the spectrum.

These spectra demonstrate that gas phases passing directly downrange contain not only atomic/molecular emissions but also disassociation/recombination products (Ca, CO, C_2, C_3) and a relatively weak thermal signal. The thermal component is reduced at large distances from the trajectory axis (FOV-2), indicating that the gas phase expanded away from fragmented projectile debris. In both solid and powdered dolomite targets, atomic emissions dominate the vapor plume along the trajectory, whereas molecular emissions characterize the plume away from the trajectory.

Layered Targets and Complex Targets: The spectral evolution for an experiment with a dusting of graphite on top of sugar and dolomite (Figure 3) exhibits similar brightening with distance (time). Spectra taken close to the impact point but off axis (FOV-1) doubled in radiance at a given wavelength at FOV-6 (along along trajectory) and FOV-4 (along the same line but opposite sides). Figure 3b reveals molecular CO and C_2 in absorption close to the impact (FOV-1). Hence, cooler gases expand along the line of sight in front of the heated ejecta (thermal) with Mg and MgO emission lines from the substrate downrange.

Conclusions and Implications: *First*, the observations from DI are most consistent with a highly porous, layered but weakly bonded target. *Second*, the higher frame-rate MRI camera on DI was critical for capturing the early evolution but it also missed the initial stages. Experiments reveal that the downrange plume (vapor, entrained dust, and condensates) rapidly expand initially but slow to the observed downrange speed (and lateral expansion rate) within the first frame, thereby producing an enigmatic offset at first appearance. *Third*, The leading edge (highest speed) of the downrange component should be primarily composed of near-surface materials (one projectile diameter). *Fourth*, Vaporization of organic rich surface materials will result in a relatively faint visible plume initially but the condensation of high-emissivity carbon-based byproducts emerging later. *Fifth*, a faint pillar-like plume directed uprange should be composed of deeper materials and could account for the "first light" [2,10]. *Sixth*, relatively pristine cometary materials should have comprised the most of what was seen by earth-based observers and non-DI probes but would have been derived from the upper few meters. *Seventh*, the long-lasting high-angle (low-speed) ejecta directly above the crater should be composed of materials from deep (>10m) within the comet during later stages of excavation. For a uniform target, the ejecta curtain should be a mixture of all stratigraphic horizons. If the a competent substrate exists below, however, then it should be primarily comprised of upper (5m) surface materials.

References: [1] A'Hearn M. F. *et al.* (2005) *Science, 310*, 258-264;[2] Schultz P. H., *et al.* (2005), *Space Sci. Rev.*, *117*, 207-239;[3] Ernst, C.M. et al. (2006), *LPS 37*, #2192; [4] Melosh, H.J., (2006), *LPS 37*, #1165; [5] Sunshine, J.M. *et al.* (2006), *LPS 37*, #1890; [6] Sugita *et al* (1998), *J. Geophys. Res.*,*103,* 19,427-19,441; [7] Schultz P.H. *et al*. (2006), *Intern. J. Impact Engin. 33*, 771-780; [8] Ahrens, T.J. *et al.* (1971), *Jour. of Appl. Phys.*, *42*, 815-829; [9] Schultz P. H. (1996) *J. Geophys. Res. 101*, 21,117-21,136. [10] Schultz P.H. *et al.* (2006), *LPS 37*, #2294;

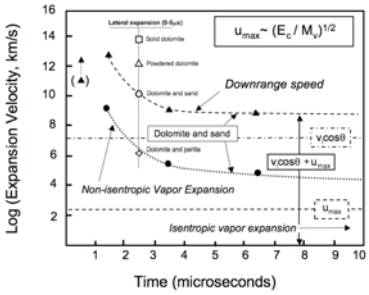

Figure 1. Evolution of vapor cloud front. Expansion velocity and downrange speed of the gas front appears to decreases during the first 10 μs due to internal shocks. At later times (50-100μs), vapor expansion approaches u_{max}, which is related to the internal energy of the cloud.

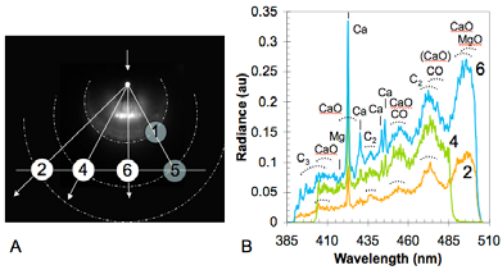

Figure 2 A. Reference image showing size and location of spectral measurements (5.9 km/s oblique impact into solid dolomite. Each dash-dotted semi-circle is schematic representation of expanding vapor plume as it travels downrange and passes the different fields of view (FOV's) over the first 50 μs. **B.** Atomic emissions disappear by the time the vapor reaches FOV-2. Near off-axis (FOV-4) and on-axis (FOV-6) indicates lateral expansion of same component.

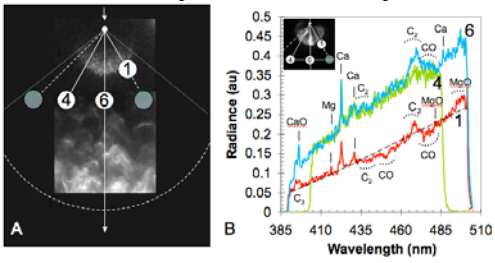

Figure 3 A. Delayed brightening of vapor plume due to condensation of carbon resulting from an oblique impact by Pyrex sphere (0.635cm) into a layer (0.318cm) of sugar over dolomite. The inset is a composite showing the early-stage plume 5 μs and 35 μs after impact. **B.** Spectra from oblique impact into a layer of sugar (0.318cm) over dolomite with a dusting of graphite on top. Spectra reveal enhanced continuum farther from the impact due to condensation of carbon.